

# Auto-alignment system design for the AEI 10 m prototype facility, 1st draft

Fumiko Kawazoe for the GEO-ISC group

April 2010

This document describes the AEI 10 m Prototype interferometer Auto-Alignment design work which was done from January to April, 2010 as part of the GEO-ISC group.



## TABLE OF CONTENTS

	Page
Chapter 1: Introduction . . . . .	1
Chapter 2: The Auto-alignment control . . . . .	2
2.1 The concept . . . . .	2
2.2 Relative alignment . . . . .	2
2.3 Gouy phase lenses . . . . .	7
2.4 Steering mirror actions . . . . .	7
2.5 Spot position control . . . . .	9
2.6 Control bandwidth . . . . .	12
2.7 summary . . . . .	12
Bibliography . . . . .	14

## Chapter 1

**INTRODUCTION**

The AEI 10 m prototype facility will provide a suitable experimental environment for interferometric experiments with their sensitivities limited by the fundamental quantum noise. One such experiments, the Sub-SQL interferometer, will be the first to be tested inside the prototype. Its design sensitivity reaches a level of  $10^{-19}$  m/ $\sqrt{\text{Hz}}$  at 50 Hz dropping to below  $10^{-20}$  Hz/ $\sqrt{\text{Hz}}$  at 1 kHz, allowing a gap between the Standard Quantum Limit by a factor of 3. Although the limiting noise sources are the suspension thermal noise, Radiation pressure noise by the intensity fluctuation of the laser, and the coating thermal noise, reducing all of the known classical noise sources is vital for meeting the required level. The laser frequency noise is the main focus of this document. In order to suppress the laser frequency noise to the required level, which is about a factor of 8 below the design sensitivity, the sub-SQL interferometer will utilize an external cavity called a frequency reference cavity. Use of the external cavity instead of utilizing its own cavity arms is necessary due to the fact that the sub-SQL interferometer will use very light mirrors with respect to the circulating power inside the arm cavities so that the arms are susceptible to radiation pressure noise. The frequency reference cavity will then provide an input laser with the frequency noise suppressed to a level of  $10^{-4}$  Hz/ $\sqrt{\text{Hz}}$  at 20 Hz dropping to below  $10^{-6}$  Hz/ $\sqrt{\text{Hz}}$  at 1 kHz. In order to achieve this level the laser frequency is locked to the frequency set by the reference cavity's optical length. However angular fluctuations of the mirrors also need to be controlled to optimize the operating point. Therefore the alignment control design has to be developed. The proposed design of the alignment control system for the reference cavity is described in this paper. From here on the system is called the auto-alignment control.

## Chapter 2

**THE AUTO-ALIGNMENT CONTROL****2.1 The concept**

The purpose of the Auto-alignment control is to obtain the increased accuracy of optimum operating conditions. The plan is to use a similar method that the GEO 600 detector uses [2], [1]. The signals necessary for the Auto-alignment system will only be available when the longitudinal degree of freedom is controlled, therefore from here on we assume that the longitudinal degree of freedom is already controlled. The optimum operating conditions are met when the alignment of the incoming beam and that of the eigenmode of the reference cavity match (this requires controlling 4 DOFs), and the absolute alignment of the cavity eigenmode is kept ideal (this requires controlling 6 DOFs). We aim to obtain such conditions by controlling the axis of the incoming beam to match the cavity eigenmode, and by controlling the beam spot positions on the cavity mirrors, respectively.

**2.2 Relative alignment**

The Differential Wavefront Sensing (DWS) scheme [2], [1] will be used for controlling the axis of the incoming beam to match the cavity eigenmode. Two split photo-detectors (QPD) placed at the reflection port are used to detect the overlap between the promptly reflected beam and the beam that is leaked from the cavity. A set of lenses will be placed in front of one of the two QPDs so that they give two different information about the misalignment; one mainly contains the information regarding lateral shifts at the waist, the other mainly angular shifts. Table 2.1, and 2.2 show how a misalignment of each cavity mirror will change the cavity eigenmode, and what type of misalignment(i.e. to which of the two QPDs the signal is sensitive). The calculations were done using the c code developed by G. Heinzl [3]. In detail, the very left column of all the tables show what mirror is misaligned and in which direction, with  $\alpha_{a,b,c}$  representing yaw misalignments of the corresponding mirrors(Ma, Mb,

and Mc), and  $\alpha_{+,-}$  representing the common and differential yaw misalignments of mirror Ma and Mc, (i.e.  $\alpha_{\pm} = (\alpha_a \pm \alpha_c)/2$ ). For pitch direction one can replace  $\alpha$  with  $\beta$ . The top row of the first table of each set show locations where a beam hits on the corresponding mirrors, with  $P_{a,b,c}$  representing the coordinate of the beam on mirror Ma, Mb, and Mc, respectively,  $\Delta x, y, z$  representing the change in each direction compared to the aligned case. The top row of the bottom tables show from left to right, the location of the waist, the angle of the outgoing beam from the cavity leak, with  $\gamma$  representing the yaw direction and  $\delta$  representing the pitch direction, the angle of the promptly reflected beam, each with respect to the aligned case, the relative angle between the beam that is leaked from the cavity and the promptly reflected beam, and the characteristic of the cavity misalignment at the waist. The characteristic of the cavity misalignment indicates the ratio between a lateral shift and a angular shift of the waist position. Due to the nature of the process of obtaining DWS signals, a signal is obtained the waist, a demodulated signal is maximized when the misalignment at the waist is the pure angular type, or  $\Theta^W = 90^\circ$ . In order to be sensitive to the pure lateral shift type of misalignment, one can modify this amount by adding  $90^\circ$  to it, by e.g. propagating the outgoing beam further, or inserting lenses. (These lenses are called Gouy phase lenses here, and they will be described in the following section.) For detailed explanation of the DWS signal processing see p.111 ~ p 115 of [2]. Figure 2.1 shows the eigenmode of the aligned cavity (top), and the eigenmode when Ma is misaligned by  $\alpha_a$  to show an example.

The two sets of two tables show that the two DOFs, namely  $\alpha_+$ , and  $\beta_-$ , will make very small signals (i.e. they will cause zero lateral shift of the waist position, and almost zero angle between the cavity leaked beam and the promptly reflected beam.) Therefore they will not be controlled by the DWS scheme. But it will be shown that they appear as spot position shifts on the QPDs, and from there the remaining two DOFs can be controlled, which will be described in the following section. (Incidentally these two DOFs are separated from the other DOFs by horizontal lines to indicate that they will not be controlled here.)

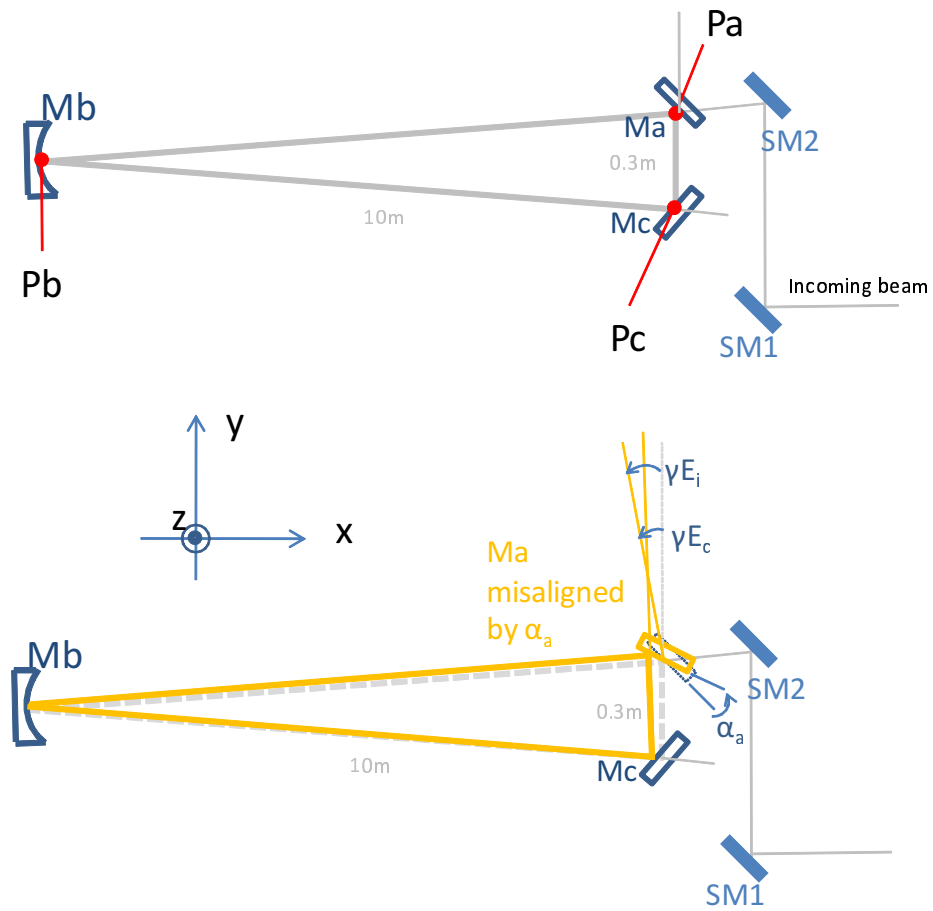


Figure 2.1: Cavity eigenmode of the aligned case and an example of a misaligned case. Here  $M_a$  is misaligned by the angle  $\alpha_a$ .

Cause	$P_a$ $\Delta x$	$P_a$ $\Delta y$	$P_b$ $\Delta y$	$P_c$ $\Delta x$	$P_c$ $\Delta y$
$\alpha_a$	$-10.202 m \cdot \alpha_a$	$10.051 m \cdot \alpha_a$	$0.205 m \cdot \alpha_a$	$-9.900 m \cdot \alpha_a$	$-9.754 m \cdot \alpha_a$
$\alpha_b$	$0.205 m \cdot \alpha_b$	$-0.202 m \cdot \alpha_b$	$-13.974 m \cdot \alpha_b$	$-0.205 m \cdot \alpha_b$	$-0.202 m \cdot \alpha_b$
$\alpha_c$	$9.900 m \cdot \alpha_c$	$-9.754 m \cdot \alpha_c$	$0.205 m \cdot \alpha_c$	$10.202 m \cdot \alpha_c$	$10.051 m \cdot \alpha_c$
$\alpha_-$	$-10.051 m \cdot \alpha_-$	$9.903 m \cdot \alpha_-$	$0.000 m \cdot \alpha_-$	$-10.051 m \cdot \alpha_-$	$-9.903 m \cdot \alpha_-$
$\alpha_+$	$-0.151 m \cdot \alpha_+$	$0.149 m \cdot \alpha_+$	$0.205 m \cdot \alpha_+$	$0.151 m \cdot \alpha_+$	$-0.149 m \cdot \alpha_+$

Cause	Waist $\Delta x$	$E_c$ $\gamma E_c$	$E_i$ $\gamma E_i$	Relative angle $\gamma E_c - \gamma E_i$	$\Theta^W$
$\alpha_a$	$-10.051 m \cdot \alpha_a$	$1.005 \cdot \alpha_a$	$2 \cdot \alpha_a$	$1.005 \cdot \alpha_a$	$59.2^\circ$
$\alpha_b$	$0.000 m \cdot \alpha_b$	$-1.370 \cdot \alpha_b$	$0 \cdot \alpha_b$	$-1.370 \cdot \alpha_b$	$-90^\circ$
$\alpha_c$	$10.051 m \cdot \alpha_c$	$1.005 \cdot \alpha_c$	$0 \cdot \alpha_c$	$-0.995 \cdot \alpha_c$	$59.5^\circ$
$\alpha_-$	$-10.051 m \cdot \alpha_-$	$0.000 \cdot \alpha_-$	$1 \cdot \alpha_-$	$-1.000 \cdot \alpha_-$	$59.4^\circ$
$\alpha_+$	$0.000 m \cdot \alpha_+$	$1.005 \cdot \alpha_+$	$1 \cdot \alpha_+$	$0.005 \cdot \alpha_+$	$90^\circ$

Table 2.1: Differential Wavefront Sensing signals-in yaw direction



Cause	$P_a$ $\Delta z$	$P_b$ $\Delta z$	$P_c$ $\Delta z$		
$\beta_a$	$-19.665 m \cdot \beta_a$	$-26.930 m \cdot \beta_a$	$-19.876 m \cdot \beta_a$		
$\beta_b$	$-37.800 m \cdot \beta_b$	$-37.800 m \cdot \beta_b$	$-37.800 m \cdot \beta_b$		
$\beta_c$	$-19.876 m \cdot \beta_c$	$-26.930 m \cdot \beta_c$	$-19.665 m \cdot \beta_c$		
$\beta_+$	$-19.770 m \cdot \beta_-$	$-26.930 m \cdot \beta_-$	$-19.770 m \cdot \beta_-$		
$\beta_-$	$0.106 m \cdot \beta_+$	$0.000 m \cdot \beta_+$	$-0.106 m \cdot \beta_+$		

Cause	Waist $\Delta z$	$E_c$ $\delta E_c$	$E_i$ $\delta E_i$	Relative angle $\delta E_c - \delta E_i$	$\Theta^W$
$\beta_a$	$-19.770 m \cdot \beta_a$	$0.702 \cdot \beta_a$	$1.43 \cdot \beta_a$	$0.728 \cdot \beta_a$	$32.02^\circ$
$\beta_b$	$37.800 m \cdot \beta_b$	$0.000 \cdot \beta_b$	$0.000 \cdot \beta_b$	$0 \cdot \beta_b$	$0^\circ$
$\beta_c$	$-19.770 m \cdot \beta_c$	$-0.702 \cdot \beta_c$	$0.000 \cdot \beta_c$	$0.702 \cdot \beta_c$	$31.08^\circ$
$\beta_+$	$-19.770 m \cdot \beta_+$	$0.000 \cdot \beta_+$	$0.714 \cdot \beta_+$	$0.714 \cdot \beta_+$	$31.52^\circ$
$\beta_-$	$0.000 m \cdot \beta_-$	$0.702 \cdot \beta_-$	$0.714 \cdot \beta_-$	$0.012 \cdot \beta_-$	$-90^\circ$

Table 2.2: Differential Wavefront Sensing signals-in pitch direction

### 2.3 Gouy phase lenses

As briefly mentioned in the following section, in order to obtain full information on the cavity misalignment one needs two QPDs, each being sensitive to the angular misalignment type and the lateral shift misalignment type, in terms of what happens at the waist. For that purpose, placing the Gouy phase lenses in front of one of the two QPDs will do. With the lenses the beam at the the QPD will acquire an additional Gouy pahse shift between the HG fundamental mode and the second higher-order mode by  $90^\circ$ . Figure 2.2 shows what kind of lenses can be used, and where they are located, and the beam radius change and the Gouy phase shift as the beam propagates through the lenses from the first waist to the QOD. The first lens is a converging lens with a focal length of  $60\text{ cm}$ , it will create a very small waist. Then placing a diverging lens (focal length of  $-3\text{ cm}$ ) a little bit before the new focus, and placing the QPD at some chosen distance away from the second lens, one can achieve a relative Gouy phase shift of  $90^\circ$  between the QPD and where the first lens is. This means, the other OPD should be placed where the first lens is, then we will have two QPDs that carry sufficient information of the cavity misalignment with respect to the incoming beam. At the same time one needs to take care so that the beam spot on the QPD is something of a usable size. Here we set the radius to be  $2\text{ mm}$ .

### 2.4 Steering mirror actions

Since our plan is to prepare two steering mirrors that are suspended as a single pendulum, and to use it as actuators for the DWS DOFs, one needs to calculate how they should be actuated. Figure 2.3 shows the concept of how the DWS signals are detected and being used to control the relative alignment via actuating on two steering mirrors.

Two QPDs are placed at the detection port. One (D2) is sensitive to the angular misalignment type, while the other (D1) is made to be sensitive to the lateral misalignment type by adjusting the Gouy phase with the use of two lenses. If we set the Gouy phase of  $90^\circ$  by the lenses the signals from the two photo-detectors will be given by

$$S_{D1} = -0.592 \cdot \alpha_- \quad (2.1)$$

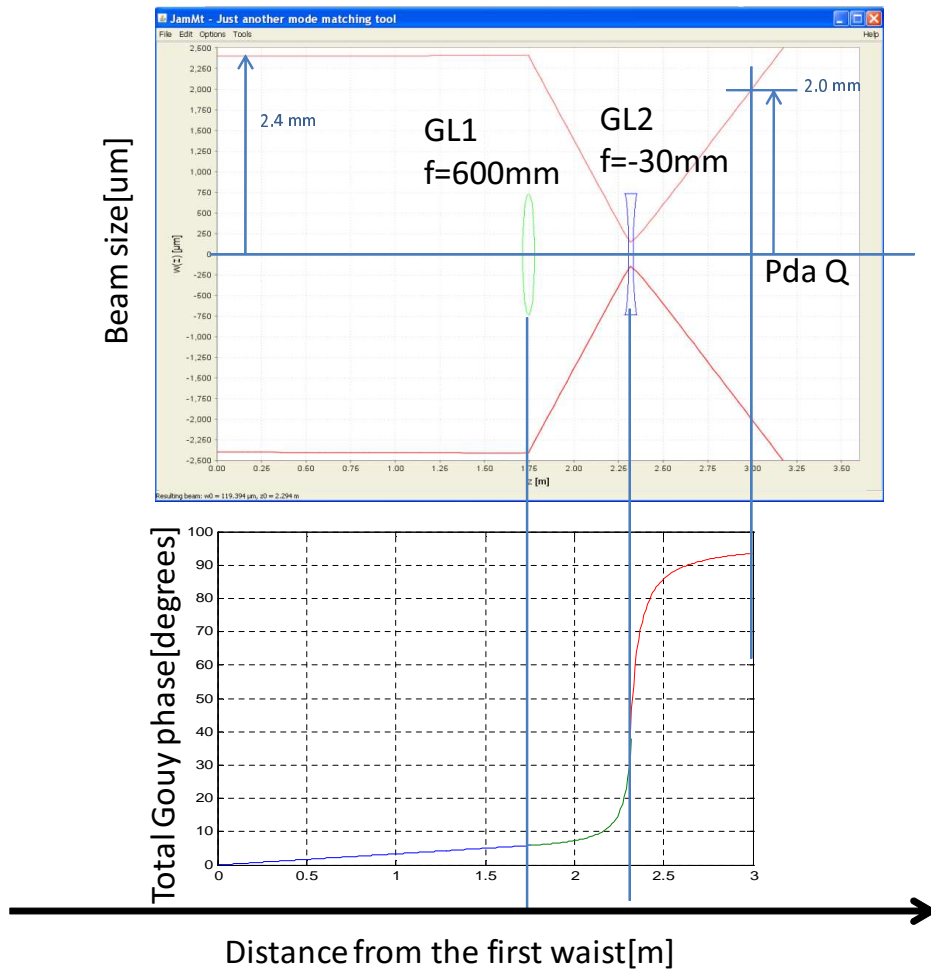


Figure 2.2: Differential Wavefront Sensing signals on two photodetectors whose Gouy phase are orthogonal to each other.

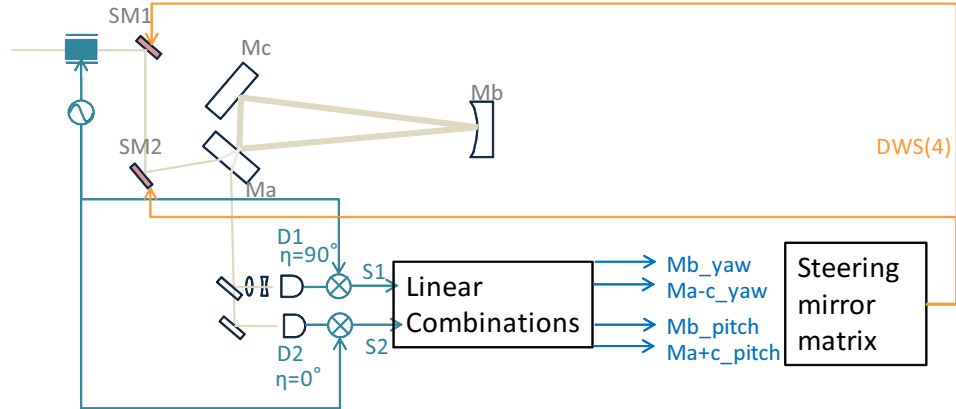


Figure 2.3: Differential Wavefront Sensing signals on two photodetectors whose Gouy phase are orthogonal to each other.

$$S_{D2} = -1.370 \cdot \alpha_b - 1.000 \cdot \alpha_- + 0.005 \cdot \alpha_+ \quad (2.2)$$

for signals in yaw direction, and

$$S_{D1} = 2.226 \cdot \beta_b - 1.164 \cdot \beta_+ \quad (2.3)$$

$$S_{D2} = -0.714 \cdot \beta_- - 0.012 \cdot \beta_- \quad (2.4)$$

for signals in pitch direction. In both directions, taking proper linear combinations will allow one to obtain four signals that are only sensitive to  $\alpha_b$ ,  $\alpha_-$ ,  $\beta_b$ , and  $\beta_+$ , since  $\alpha_+$ , and  $\beta_-$  are both very small and negligible, this will not be controlled by this method. These four signals will be multiplied by factors that are necessary for steering mirrors to be actuated properly. The factors can be found in the table below. 2.3. This was also simulated by the c code.[3]

## 2.5 Spot position control

So far we have seen that the four DOFs can be controlled by the DWS scheme. The remaining six DOFs should also be controlled. For that, three QPDs will be used to detect the spot positions. One (PD2) is placed at the back of the second steering mirror (SM2), another (PDb) at the back Mb, and the other being one of the QPDs whose AC part of the signals are already in use for the DWS scheme. Out of the two, one that has the lenses

Cause	SM1 yaw	SM2 yaw	SM1 pitch	SM2 pitch
$\alpha_b$	$0.146 \cdot \alpha_b$	$0.831 \cdot \alpha_b$	$0.000 \cdot \alpha_b$	$0.000 \cdot \alpha_b$
$\alpha_-$	$9.070 \cdot \alpha_-$	$9.570 \cdot \alpha_-$	$0.000 \cdot \alpha_-$	$0.000 \cdot \alpha_-$
$\beta_b$	$0.000 \cdot \beta_b$	$0.000 \cdot \beta_b$	$46.904 \cdot \beta_b$	$-46.558 \cdot \beta_b$
$\beta_+$	$0.000 \cdot \beta_+$	$0.000 \cdot \beta_+$	$24.267 \cdot \beta_+$	$-23.588 \cdot \beta_+$

Table 2.3: Steering mirror matrix

inserted in the path will be used, due to the fact that it is likely to be more sensitive due to the magnification set by the lenses (however it is not always so, because a general misalignment is a mixture of a lateral shift and the angular shift, and depending upon how they are combined, one can get a reduced signal due to the lenses). Tables 2.4, and 2.5 show how the cavity mirrors misalignment will cause spot positions to change. Pda I, and Pda Q are the ones that are used for the DWS signals, with Pda Q having lenses inserted in the beam path. Pdc is placed behind Mc, but currently it is not planned to be used, due to the fact that it is not necessary, however it is also listed here for a comparison purpose. The QPD locations can be found in Fig.2.4.

Cause	PD2	Pda I	Pda Q	PDb	(Pdc)
$\alpha_a$	$13.106 m \cdot \alpha_a$	$11.861 m \cdot \alpha_a$	$10.206 m \cdot \alpha_a$	$-0.072 m \cdot \alpha_a$	$-10.027 m \cdot \alpha_a$
$\alpha_b$	$0.227 m \cdot \alpha_b$	$-2.426 m \cdot \alpha_b$	$-18.977 m \cdot \alpha_b$	$14.194 m \cdot \alpha_b$	$-0.033 m \cdot \alpha_b$
$\alpha_c$	$-12.697 m \cdot \alpha_c$	$-8.270 m \cdot \alpha_c$	$17.645 m \cdot \alpha_c$	$-0.341 m \cdot \alpha_c$	$10.356 m \cdot \alpha_c$
$\alpha_+$	$0.205 m \cdot \alpha_+$	$1.796 m \cdot \alpha_+$	$13.926 m \cdot \alpha_+$	$-0.207 m \cdot \alpha_+$	$0.165 m \cdot \alpha_+$
$\alpha_-$	$12.902 m \cdot \alpha_-$	$10.065 m \cdot \alpha_-$	$-3.720 m \cdot \alpha_-$	$0.135 m \cdot \alpha_-$	$-10.192 m \cdot \alpha_-$

Table 2.4: Spot positioning signal for yaw direction

Similar to the DWS signal case, adding and subtracting signals from various QPDs will allow one to form a linearly independent signal that are clean in terms of signal mixture. Such combinations are shown in the following equations.

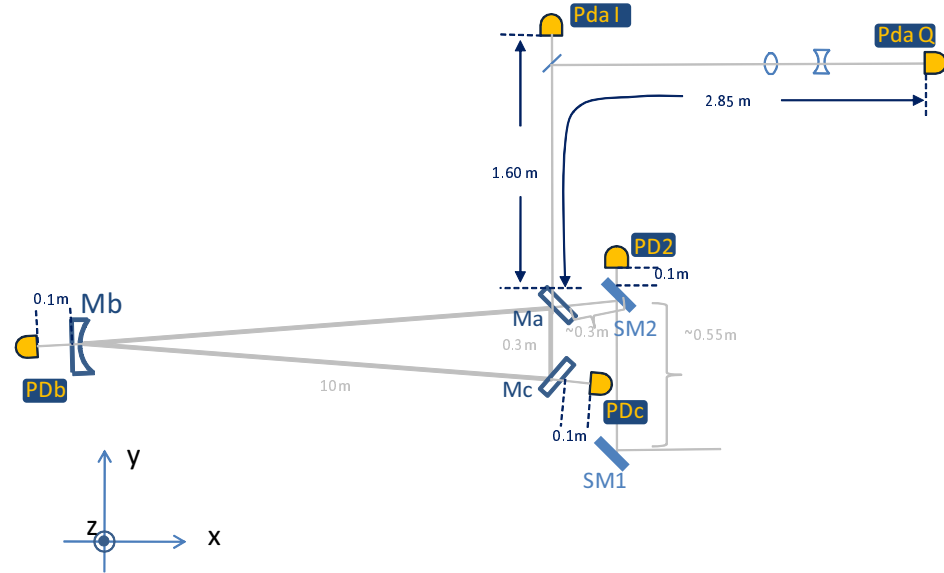


Figure 2.4: Spot positioning signals on three photodetectors.

Cause	PD2	PDa I	PDa Q	PDb	(PDC)
$\beta_a$	$24.706 m \cdot \beta_a$	$18.496 m \cdot \beta_a$	$-17.020 m \cdot \beta_a$	$27.071 m \cdot \beta_a$	$19.778 m \cdot \beta_a$
$\beta_b$	$48.068 m \cdot \beta_b$	$37.800 m \cdot \beta_b$	$-13.969 m \cdot \beta_b$	$37.845 m \cdot \beta_b$	$37.800 m \cdot \beta_b$
$\beta_c$	$25.010 m \cdot \beta_c$	$21.023 m \cdot \beta_c$	$2.415 m \cdot \beta_c$	$27.068 m \cdot \beta_c$	$19.542 m \cdot \beta_c$
$\beta_+$	$24.858 m \cdot \beta_+$	$19.760 m \cdot \beta_+$	$-7.303 m \cdot \beta_+$	$27.070 m \cdot \beta_+$	$19.660 m \cdot \beta_+$
$\beta_-$	$-0.152 m \cdot \beta_-$	$-1.264 m \cdot \beta_-$	$-9.718 m \cdot \beta_-$	$0.002 m \cdot \beta_-$	$0.118 m \cdot \beta_-$

Table 2.5: Spot positioning signal for pitch direction

$$SP_{\alpha_b} = 1.000 \cdot \text{PDb} \quad (2.5)$$

$$SP_{\alpha_+} = 0.206 \cdot \text{PD2} + 0.750 \cdot \text{PDaQ} + 1.000 \cdot \text{PDb} \quad (2.6)$$

$$SP_{\alpha_-} = 1.000 \cdot \text{PD2} \quad (2.7)$$

$$SP_{\beta_b} = 2.830 \cdot \text{PD2} - 0.045 \cdot \text{PDaQ} - 2.611 \cdot \text{PDb} \quad (2.8)$$

$$SP_{\beta_+} = -0.291 \cdot \text{PD2} + 0.05 \cdot \text{PDaQ} + 0.371 \cdot \text{PDb} \quad (2.9)$$

$$SP_{\beta_-} = 0.291 \cdot \text{PD2} + 1.000 \cdot \text{PDaQ} \quad (2.10)$$

Each combination will contain one DOF, that can be applied to the cavity mirrors accordingly to realize the spot position control.

## **2.6 Control bandwidth**

to be filled

## **2.7 summary**

The table 2.6 summarizes the concept of the control system and reasons behind them.

Table 2.6: Concept

	Method	Action	bandwidth	Reason
Relative alignment	DWS	Actuate on two steering mirrors to overlap the promptly reflected beam and the beam leaking from the cavity	-	To obtain fast enough action, a steering mirror, which is suspended as a single pendulum serves as more suitable actuator than a cavity mirror, which is suspended as a triple pendulum
Beam position on mirrors	Spot position	Actuate on cavity mirrors	-	Steering mirrors are in use already for the DWS.



**BIBLIOGRAPHY**

- [1] H Grote. *Making it Work: Second Generation Interferometry in GEO600 !* PhD thesis, University of Hannover, 2003.
- [2] G Heinzl. *Advanced optical techniques for laser-interferometric gravitational-wave detectors.* PhD thesis, University of Hannover, 1999.
- [3] ifocad by G. Heinzl. simulation tool, 2010.